

# Dynamics of Kicked and Accelerated Massive Black Holes in Galaxies

David A. Kornreich<sup>1</sup>

*Department of Physics and Astronomy, Humboldt State University, Arcata, CA 95521*  
and

Richard V. E. Lovelace

*Departments of Astronomy and Applied and Engineering Physics, Cornell University, Ithaca, NY 14850*

## ABSTRACT

A study is made of the behavior of massive black holes in disk galaxies that have received an impulsive kick from a merger or a sustained acceleration from an asymmetric jet. The motion of the gas, stars, dark matter, and massive black hole are calculated using the GADGET-2 simulation code. The massive black hole escapes the galaxy for kick velocities above about  $600 \text{ km s}^{-1}$  or accelerations above about  $4 \times 10^{-8} \text{ cm s}^{-2}$  over time-scales of the order of  $10^8 \text{ yr}$ . For smaller velocity kicks or smaller accelerations, the black hole oscillates about the center of mass with a frequency which decreases as the kick velocity or acceleration increases. The black hole displacements may give rise to observable nonaxisymmetries in the morphology and dynamics of the stellar and gaseous disk of the galaxy. In some cases the dynamical center of the galaxy is seen to be displaced towards the direction of the BH acceleration with a characteristic “tongue-” shaped extension of the velocity contours on the side of the galaxy opposite the acceleration.

*Subject headings:* galaxies: kinematics and dynamics — galaxies: structure — galaxies: nuclei

## 1. Introduction

Recent breakthroughs in numerical General Relativity have led to predictions of large recoil velocities of merged binary black-holes (BHs) as the binary radiates away linear momentum as gravitational waves during the final stages of merger (González *et al.* (2007), Campanelli *et al.* (2007)). The velocity or “kick” of the merged black-hole in the nucleus of a galaxy can be as large as  $4000 \text{ km s}^{-1}$ , which would be more than enough to eject the BH from the galaxy. However, it is more likely that typical kick velocities are much smaller ( $\lesssim 200 \text{ km s}^{-1}$ ) owing to gas accretion by

the merging BHs and a large ratio of the masses of the two initial BHs (Bogdanović *et al.* 2007).

In another situation, the asymmetric or one-sided jet from the disk around a massive BH can give a steady acceleration of the black hole over the Salpeter time-scale  $\sim 10^8 \text{ yr}$  (Shklovsky (1982); Tsygan (2007)) and this may push the BH out of the galaxy. Wang *et al.* (1992) pointed out that some combinations of dipole and quadrupole symmetry magnetic field components threading the accretion disk of the BH can give a much stronger magnetically driven jet on one side of the disk than on the other. It is of interest that a bright quasar has been discovered which is *not* inside a massive galaxy (Magain *et al.* 2005) and so it may have been ejected from a galaxy.

Field galaxies themselves may be morphologically or dynamically nonaxisymmetric even in the absence of tidal companions (Baldwin *et al.*

<sup>1</sup>Visiting Astronomer, Arecibo Observatory. The Arecibo Observatory is part of the National Astronomy and Ionosphere Center, which is operated by Cornell University under a cooperative agreement with the National Science Foundation

1980). Up to 30% of field galaxies are nonaxisymmetric (Kornreich *et al.* (1998), Zaritsky & Rix (1997)). If central supermassive BHs receive impulses from mergers or asymmetric jets, causing motion in the host galaxy, some of that motion may be transmitted to the galaxy via dynamical friction. We may expect that in such galaxies, morphological or dynamical effects may be seen in the stellar or gas distribution as a result of this transfer of momentum.

The objective of this work is to determine the BH displacement as a function of time for different initial kick velocities and directions, different accelerations due to a one sided jet, and different BH masses. A second objective is to study influence the BH displacement has on the morphology and the kinematics of the host galaxy and determine whether nonaxisymmetries in disk galaxies are attributable to motions of the BH. We have chosen to concentrate on the morphology of disk galaxies rather than ellipticals because the dynamics of disk galaxies, being supported by bulk rotation rather than random motions, are more likely to exhibit signs of disturbance if the motion of the BH interferes with that rotation.

Section 2 of the paper describes the initial conditions and the numerical methods used. Section 3 discusses the results, first for the case of velocity kicks of a  $10^8 M_\odot$  BH, and then of a  $10^9 M_\odot$  BH. Section 4 discusses the results for cases of one-sided jets, first for the  $10^8 M_\odot$  BH, and then for the  $10^9 M_\odot$  BH. Section 5 gives the conclusions of this work.

## 2. Numerical Methods and Initial Conditions

The computations for this experiment were performed using the N-body, Smoothed Particle Hydrodynamics (SPH) GADGET-2 code of Springel (2005). We have added the ability to assign a particular particle an arbitrary acceleration, in addition to the calculated gravitational acceleration, in order to simulate forces due to an asymmetric jet. This particle is given significant mass and placed initially at the center of the galaxy.

The considered galaxy consists of a dark halo, a stellar disk and bulge, and a gas disk. The gas particles are treated gravitationally and hydrodynamically, while the other particles interact

gravitationally. The halo, disk, and bulge particles differ in mass and spatial distribution, but are otherwise treated identically in the computation. The central stellar bulge is modeled as a Plummer (1915) sphere, which has a density distribution of a relaxed  $n = 5$  polytrope given by:

$$\rho(r) = \frac{3}{4\pi} \frac{M_B}{R_B^3} \frac{1}{\left[1 + (r/R_B)^2\right]^{5/2}}, \quad (1)$$

with bulge scale radius  $R_B = 1$  kpc and mass  $M_B = 10^{10} M_\odot$ .

This bulge is placed at the center of a softened isothermal dark matter halo of density profile

$$\rho(r) = \frac{\rho_0}{1 + (r/r_c)^2}, \quad (2)$$

total mass  $5.6 \times 10^{11} M_\odot$ , with a cutoff radius 50 kpc, and core radius  $r_c = 2$  kpc. A stellar and gas disk of scale radius  $r_0 = 3.5$  kpc and cutoff radius  $R = 50$  kpc of exponential surface density

$$\Sigma(r) = \frac{M_D}{2\pi r_0^2 [1 - e^{-R/r_0} (1 + R/r_0)]} e^{-r/r_0} \quad (3)$$

surrounds the bulge with total mass  $M_D = 2.8 \times 10^{10} M_\odot$ , at a gas mass fraction of 25%. In the vertical direction, the disk particles are given velocity dispersions and uniformly random initial positions corresponding to a disk of 1 kpc thickness.

The total dynamical mass of the galaxy model is therefore  $M_{\text{tot}} = 5.98 \times 10^{11} M_\odot$ . This model was chosen to conform to parameters observed in giant disk galaxies such as those described by Rownd *et al.* (1994) and Dickey *et al.* (1990), in particular, a circular velocity of 220 km/s with a 10 km/s velocity dispersion in the disk. The total number of simulation particles used in the model was  $2 \times 10^6$  for most model runs.

In one sequence of runs, we gave the central black hole an initial impulsive velocity “kick” to simulate the recoil from the merging of two black holes. In one sequence, the kick was in the plane of the galaxy, and in the other, it was normal to the galaxy plane. The black hole was given no further acceleration. In another sequence of runs, the BH was given a steady acceleration of order  $10^{-8} \text{ cm s}^{-1}$  for a time of the order of the Salpeter time in order to simulate the influence of a one-sided jet. Each of these sequences was run for

a BH mass of  $10^8 M_\odot$  and a larger black hole of  $10^9 M_\odot$ .

During each run, the position, velocity, and acceleration of the BH was output for each timestep. Data dumps containing positions, velocities, accelerations, and (for the gas particles) temperatures were generated periodically, usually every 0.01 Gyr of simulation time. These data were read into the IDL data processing environment, where it was possible to display the results as seen from a variety of viewing angles. For a given viewing angle, gas particles were convolved with a Gaussian simulated telescope beam and displayed as logarithmic intensity contours overlaid on a diagram of stellar particle positions. Gas velocities were similarly convolved and used to produce radial velocity maps.

Additional sample runs were conducted with isothermal halo core radius 0.5 kpc, with no radius, and with the halo density profile of Navarro *et al.* (1997). In each of these cases, the results were similar and the details of the behavior did not substantially depend on the nature of the halo density profile.

### 3. Velocity “Kicks”

#### 3.1. Black Hole Mass $10^8 M_\odot$

In this series of model runs, the BH was placed near the center of mass of the galaxy and given an initial velocity in the plane of the disk. The series of initial velocities started at zero and progressed in increments of  $50 \text{ km s}^{-1}$  up to a velocity of  $650 \text{ km s}^{-1}$ , for which the central BH escaped the galaxy. It is interesting to note that this critical kick velocity is significantly larger than the escape velocity of the center of the galaxy, which was measured to be  $450 \text{ km s}^{-1}$ . We attribute this excess to dynamical friction.

The general behavior of the BH after receiving the kick was to oscillate about the model center of mass approximately sinusoidally (Figure 1). The amplitude and frequency of the motion remain roughly constant over a period of 0.5 Gyr, but depend on the kick magnitude as shown in Figure 2. Error bars represent the  $1\sigma$  standard deviation of these values as calculated for each cycle. For kick velocities below  $400 \text{ km s}^{-1}$ , the relation between amplitude and initial velocity  $V_0$  is linear, with  $A(V_0)/\text{kpc} = (9.30 \pm 0.53) \times$

$10^{-3} V_0/\text{km s}^{-1} + (0.088 \pm 0.082)$ . For initial velocities above  $400 \text{ km s}^{-1}$ , the BH amplitude is beyond the visible disk and becomes exponentially large until it escapes at  $650 \text{ km s}^{-1}$ . The frequency of the oscillation is also linear with  $f(V_0)/\text{Gyr}^{-1} = (17.64 \pm 0.57) - (0.0317 \pm 0.0015) V_0/\text{km s}^{-1}$ .

Smaller kicks resulted in the BH remaining in the more massive parts of the galaxy within 10 kpc for their entire cycles, allowing momentum from the kick to be efficiently transferred to the galaxy via dynamical friction. In these cases, damping of the oscillation was on timescales of 0.7 Gyr. The galaxy center of mass thus gained velocity in the direction of kick, resulting in the offsets depicted in the low kick amplitude curves in Figure 2. Larger kicks, while imparting greater momentum to the BH, caused it to spend a great deal of time in the thin regions of the galaxy beyond  $r = 10 \text{ kpc}$ . This greatly reduces the efficiency of the dynamical friction, lengthening damping timescales to 2.0 Gyr and reducing the momentum transferred to the galaxy.

With the frequency of the BH motion  $\omega = 2\pi f$  known as a function of the amplitude of its motion, we can derive the effective potential for its motion,  $U_{\text{eff}}$ . For a one-dimensional oscillator,

$$R = \frac{1}{\sqrt{2}} \int_0^{U_{\text{eff}}} \frac{dE}{\omega(E)\sqrt{U_{\text{eff}} - E}}, \quad (4)$$

(Landau & Lifshitz 1960). A first approximation to our simulation results gives  $\omega = \omega_0(1 - V_0/V_m)$ , where  $V_0$  is the BH kick velocity such that  $E = V_0^2/2$ , and where  $\omega_0$  and  $V_m$  are constants characteristic of the galaxy. For this dependence, equation (4) can be integrated to give

$$R' = \frac{2}{\sqrt{1 - U'}} \times \left[ \tan^{-1} \left( \frac{1 - \sqrt{U'}}{\sqrt{1 - U'}} \right) + \tan^{-1} \left( \frac{\sqrt{U'}}{\sqrt{1 - U'}} \right) \right] - \frac{\pi}{2}, \quad (5)$$

where  $R' \equiv R/R_0$ ,  $R_0 \equiv V_m/\omega_0$  and  $U' \equiv U_{\text{eff}}/(V_m^2/2)$ . For the case of Figures 1 and 2,  $V_m \approx 555 \text{ km s}^{-1}$ ,  $\omega_0 \approx 3.51 \times 10^{-15} \text{ s}^{-1}$ , and  $R_0 \approx 5.13 \times 10^3 \text{ kpc}$ . Of course, for  $V_0 \ll V_m$ ,  $U_{\text{eff}} = (1/2)\omega_0^2 R^2$  to a good approximation. Figure 3 shows this function and its derivative which is the negative of the effective force, in contrast

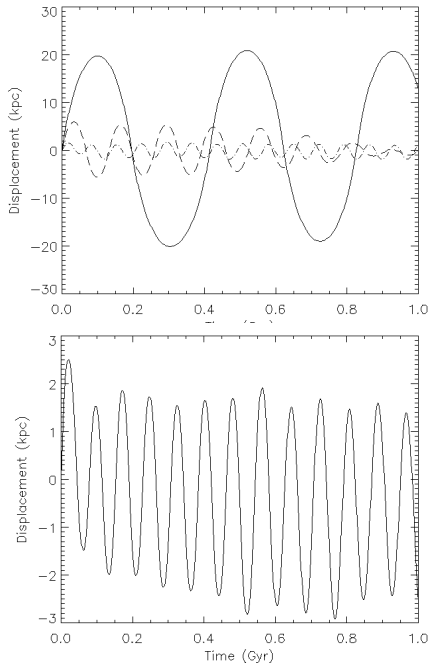


Fig. 1.— The top panel shows the motion along the direction of kick (in the plane of the galaxy) for a BH of mass  $10^8 M_\odot$  for an initial velocity kick of  $500 \text{ km s}^{-1}$  (solid line),  $350 \text{ km s}^{-1}$  (dashed line), and  $150 \text{ km s}^{-1}$  (dash-dot line). The bottom panel is for an initial kick velocity  $200 \text{ km s}^{-1}$ .

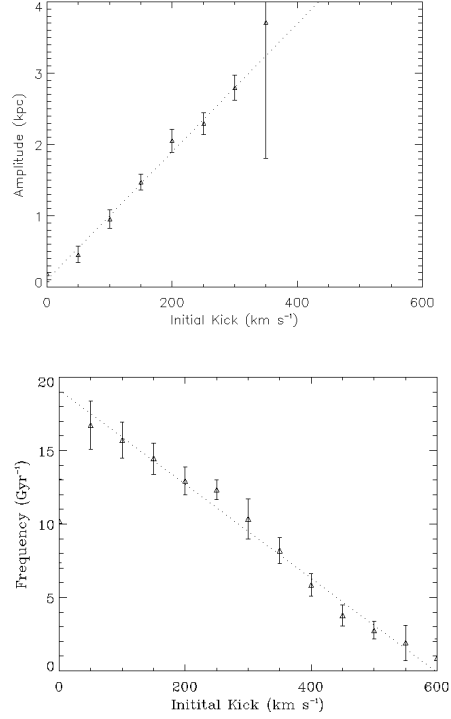


Fig. 2.— Amplitudes and frequencies of the central BH motion resulting from velocity kicks in the plane of the galaxy for a  $10^8 M_\odot$  BH.

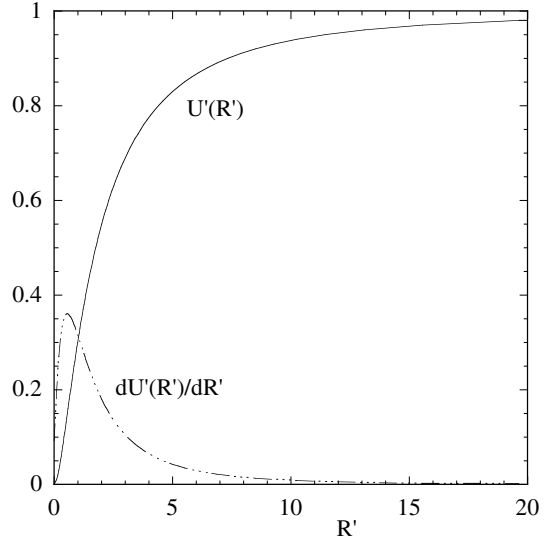


Fig. 3.— Effective potential for the BH as it oscillates about the galaxy center of mass after receiving an impulsive kick. The effective restoring force is  $\propto -dU'_{\text{eff}}/dR'$ . The maximum of the force is  $\approx 0.36$  at a distance  $R' \approx 0.56$ .

to the purely logarithmic potential of the halo isothermal sphere.

We have taken an example frame from the  $300 \text{ km s}^{-1}$  model run, inclined it to the line of sight, and convolved the gas component with a Gaussian beam. The result is Figure 4 which depicts the morphology and kinematics of the radio gas component of our galaxy model. Although the central BH is in motion, observable effects on the host galaxy are minimal. The simulated HI gas is distributed axisymmetrically, for instance. Moreover, as can be seen from the figure, lines of constant radial velocity are straight and parallel through the dynamical center of the galaxy, indicating pure rotation with little or no streaming motion, even though the central BH is clearly displaced from the dynamical center of the galaxy. This is the behavior we observed throughout this set of runs.

A series of runs was also conducted with the velocity kick normal to the plane of the galaxy. Qualitative results were similar to the case where the kick is in the plane of the galaxy, with the BH oscillating roughly sinusoidally through the center of mass. The amplitude–initial kick relation remains linear for a slightly smaller range of kicks, however (Figure 5). For velocity kicks less than  $350 \text{ km s}^{-1}$ , the amplitude–initial kick relation is:  $A(V_0)/\text{kpc} = (8.06 \pm 0.51) \times 10^{-3} V_0/\text{km s}^{-1} + (0.126 \pm 0.067)$ , making the linear part of the amplitude–kick relation independent of direction to within  $2\sigma$ . Again, escape from the galaxy occurs for an initial kick  $650 \text{ km s}^{-1}$ .

As in the coplanar case, little disturbance of the morphology and kinematics of the stellar or gas disk is observed; only a displacement of the BH from the center of the galaxy disk is observed. However, when viewed nearly face-on, some streaming motions are observed in the gas kinematics, as illustrated in Figure 6.

### 3.2. Black Hole Mass $10^9 M_\odot$

When receiving an impulsive initial velocity “kick,” a large  $10^9 M_\odot$  black hole exhibits qualitatively similar behavior to the  $10^8 M_\odot$  black hole, as shown in Figure 7. In this case, however, it is clear that the damping time of the oscillation is significantly shorter. In the  $10^8 M_\odot$  case, the damping scale time was on the order of 1.5 Gyr;

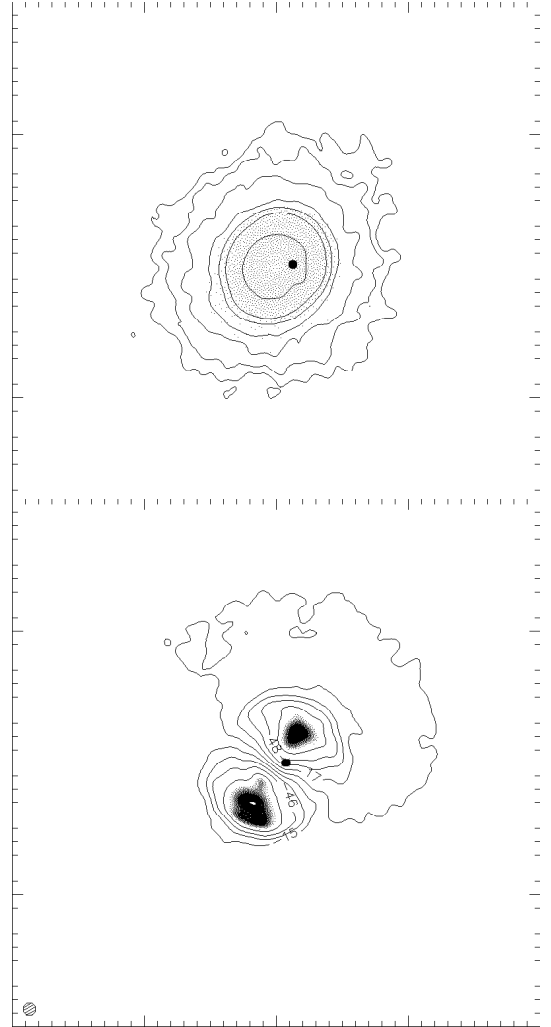


Fig. 4.— Morphology and kinematics of the galaxy model at  $t = 0.12 \text{ Gyr}$  after the central BH of mass  $10^8 M_\odot$  has been given a velocity kick of  $300 \text{ km s}^{-1}$  in the plane of the galaxy. In the top panel, the stellar disk is illustrated in greyscale and the logarithmic contour lines indicate density of HI gas, after convolution with a simulated Gaussian beam (lower left). In the lower panel, the convolved radial velocity of the gas is indicated by the contour lines, labeled in  $\text{km s}^{-1}$ . The inclination to the line of sight is  $20^\circ$ . In both diagrams, the BH is indicated by the black dot slightly to the right of center. Major tick marks delineate 25 kpc.

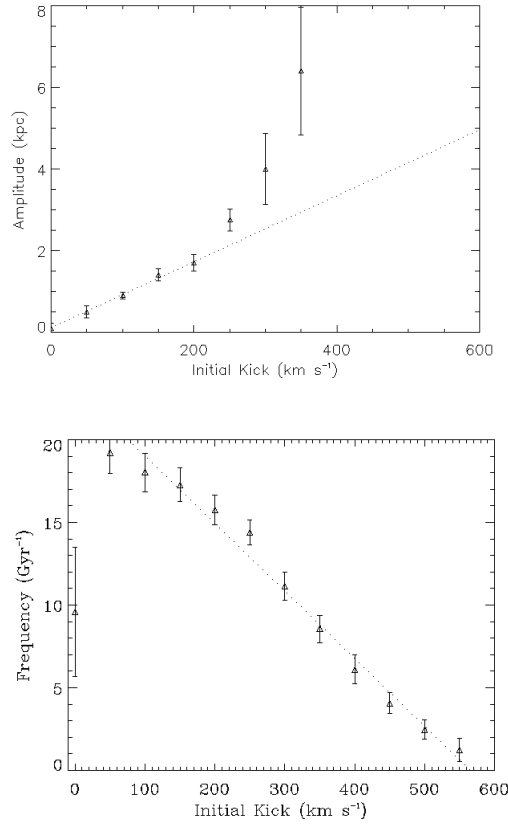


Fig. 5.— Amplitudes and frequencies of the BH motion resulting from velocity kicks perpendicular to the plane of the galaxy for a BH of mass  $10^8 M_{\odot}$ .

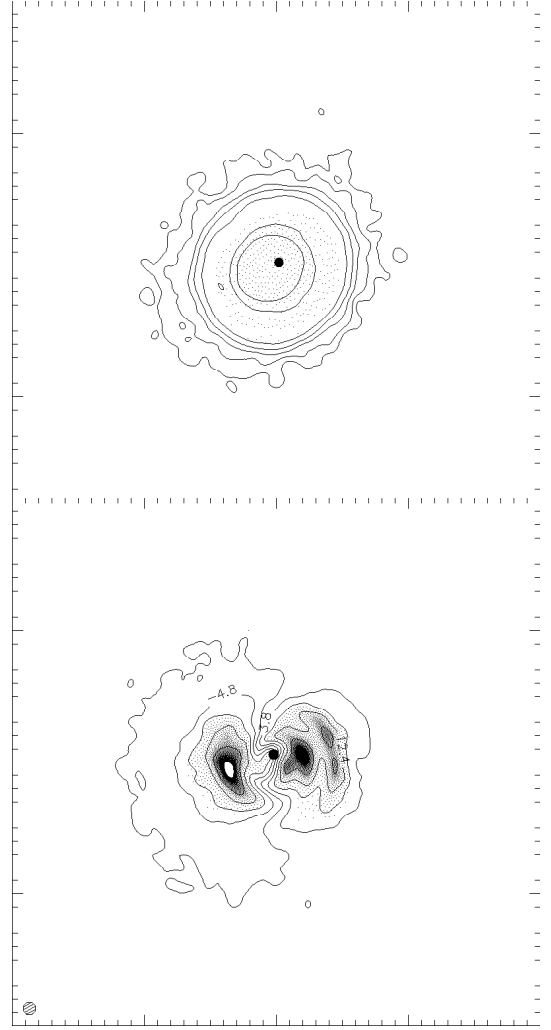


Fig. 6.— Morphology and Kinematics of the galaxy model at  $t = 0.70$  Gyr after the central BH has been given a velocity kick of  $300 \text{ km s}^{-1}$  perpendicular to the plane of the galaxy for a BH of mass  $10^8 M_{\odot}$ . In the top panel, the stellar disk is illustrated in greyscale and the logarithmic contour lines indicate density of HI gas, after convolution with a simulated Gaussian beam (lower left). In the bottom panel, the convolved radial velocity of the gas is indicated by the contour lines labeled in  $\text{km s}^{-1}$ . The inclination to the line of sight is  $10^\circ$ . In both panels the BH is indicated by the black dot in the center. Major tick marks delineate 25 kpc.

however, for the  $10^9 M_\odot$  case, damping times are of the order of 0.8 Gyr.

During the period of significant motion of the black hole, significant dynamical disturbance can be detected in the HI velocity maps. After a damping scale time, however, the dynamics recover to a normal rotation curve. Morphology outside the disk scale radius remains generally undisturbed, although minor observable asymmetries occasionally appeared in the central gas distribution. Despite the normal disk and gas morphology, however, as in the previous case, the central black hole could be found offset from the center of the disk by several kpc.

Typical induced kinematic asymmetries are presented in Figure 8. In these plots, gas particle velocities were convolved and combined in a simulated Gaussian telescope beam and lines of constant radial velocity drawn. If the galaxy were a symmetric rotator, then constant radial velocity lines should be straight and parallel as they pass through the dynamical center. However, as can be seen in the figure, these kinematics have been disturbed by the motion of the BH, which has resulted in a dynamical friction interaction with the galaxy. The central regions of the galaxy, within the disk scale radius of 3.5 kpc react quickly to the transferred momentum of the BH, and tend to move with it in its direction of motion. Beyond that radius, particles are shielded from the gravity of the central BH and react sluggishly. As a result, the dynamical center of the central galaxy is displaced from the overall dynamical center in the direction of the initial impulse given to the BH. In the transition region between the two regimes, streaming motions are evident, with magnitudes on the order of  $30 \text{ km s}^{-1}$ . Finally, because of the BH's resulting orbit around the new dynamical center of the distribution, at most times its actual location was offset from the dynamical center as in the second frame of Figure 8.

#### 4. BH Acceleration Due to a One-Sided Jet

In order to simulate the influence of a one-sided jet, we did a series of runs where the massive BH was placed in the center of the galaxy with zero initial velocity relative to the galaxy, but with an applied constant acceleration for a time of the

order of the Salpeter time. The available accretion power from a BH is  $L_a = \epsilon \dot{M}_a c^2$  where  $\dot{M}_a$  is the mass accretion rate and the efficiency is assumed to be  $\epsilon = 0.1$ . Usually, the accretion rate is measured in units of the rate which would give the Eddington luminosity for the BH, that is  $\dot{M}_{\text{Edd}} = L_{\text{Edd}}/(\epsilon c^2) \approx 2.2(M_{bh}/10^8 M_\odot) M_\odot \text{yr}^{-1}$ , where  $L_{\text{Edd}} \approx 1.26 \times 10^{46} (M_{bh}/10^8 M_\odot) \text{ erg/s}$  and  $M_{bh}$  is the BH mass. Thus, the accretion luminosity can be written as  $L_a = \dot{m} L_{\text{Edd}}$ , where  $\dot{m} \equiv \dot{M}_a/\dot{M}_{\text{Edd}}$ . The exponentiation time of the BH mass growth, the Salpeter (1964) time, is  $T_S \approx 4.5 \times 10^7 \dot{m}^{-1} \text{ yr}$ .

It is widely thought that the jets of active galaxies are due to the presence of a strong, ordered magnetic field ( $\sim 10^3\text{--}10^4 \text{ G}$ ) threading the BH accretion disk. For the commonly considered case of a field with dipole symmetry the magnetically driven jets are of equal strength on the two sides of the disk (Lovelace 1976). However, as Wang *et al.* (1992) pointed out, an ordered field in the disk consisting of *dipole* and *quadrupole* components can give magnetically driven jets of unequal strength on the two sides of the disk. In fact, one side of the disk may have a dominant jet. The timescale for the jet to be on one side  $\tau$  in this model is of the order of the time for plasma and magnetic field to move through the disk. This time may be shorter than  $T_S$ . Nevertheless, we emphasize in our simulations the influence of a one-sided jet by maintaining its force on the BH for a time of the order of  $T_S$  after which the force is zero. We assume that the BH carries along with it bound gas and stars sufficient to supply  $\dot{M}_a$  during this time.

For the case of a one-sided jet, we can write the jet luminosity as  $L_{\text{jet}} = f_{\text{jet}} L_a$ , where  $f_{\text{jet}} \leq 1$  is the fraction of the accretion luminosity going into the jet. Alternatively, for asymmetrical, oppositely directed jets we take  $L_{\text{jet}}$  to be the *difference* in the luminosities of the two jets. Assuming that the jet outflow is highly relativistic, the force on the BH/disk system is therefore

$$F_{bh} = -L_{\text{jet}}/c \approx 4.2 \times 10^{35} f_{\text{jet}} \dot{m} \left( \frac{M_{bh}}{10^8 M_\odot} \right) \text{ dynes}, \quad (6)$$

and the BH acceleration is

$$a_{bh} = \frac{|F_{bh}|}{M_{bh}} \approx 2.1 \times 10^{-6} f_{\text{jet}} \dot{m} \frac{\text{cm}}{\text{s}^2}, \quad (7)$$

(Wang *et al.* 1992). The momentum imparted to the BH during a time  $T$  is  $I = \int_0^T dt M_{bh} a_{bh} = T M_{bh} a_{bh}$  for constant one-sided jet. For a jet which changes sides randomly on a timescale  $\tau \ll T$ , the imparted momentum is much smaller,  $I \sim (\tau T)^{1/2} M_{bh} a_{bh}$ . The small values of the BH displacements estimated by Wang *et al.* (1992) resulted from an invalid assumption about the rigidity of the central potential of the galaxy.

As a reference value for our simulations, we take  $a_{bh} = 2 \times 10^{-8} \text{ cm s}^{-1}$  which corresponds to  $f_{\text{jet}} \dot{m} = 0.01$ . For this value of  $a_{bh}$ , notice that  $\int_0^T dt a_{bh} = T a_{bh} \approx 1260(T/2 \times 10^8 \text{ yr}) \text{ km s}^{-1}$ . We confirmed the relevance of this value by observing that the hole remains bound to the galaxy for applied accelerations up to  $a_{bh} = 4.5 \times 10^{-8} \text{ cm s}^{-2}$ , and escapes the galaxy for larger  $a_{bh}$ . A hundred times larger value of  $a_{bh}$  was considered by Tsygan (2007) to apply over a time scale  $T_S$  and this will strongly eject the BH from the galaxy.

#### 4.1. Black Hole Mass $10^8 M_\odot$

When an external acceleration was applied in the plane of the galactic disk, the typical behavior was for the  $10^8 M_\odot$  BH to find an equilibrium position off-center of the morphological and dynamical center of the galaxy and to oscillate about that position as long as the acceleration was applied. Figure 9 illustrates the BH displacement as a function of time for two typical examples of this experiment, in which the  $10^8 M_\odot$  black hole was given an applied acceleration of  $2.0 \times 10^{-8} \text{ cm s}^{-1}$  and  $4.0 \times 10^{-8} \text{ cm s}^{-1}$  in the plane of the galaxy. The center of mass of the galaxy is also depicted for the first experiment. This accelerates as well, as dynamical friction transfers momentum between BH and the galaxy. In the second run, the BH escapes the galaxy entirely within 0.1 Gyr. In each run where the BH remained bound, we confirmed that the acceleration of the center of mass of the galaxy was equal to  $a_{bh}(M_{bh}/M_{\text{tot}})$ , where  $a_{bh}$  was the acceleration imparted to the BH, and also that when  $a_{bh}$  was turned off after 200 Myr, that the final velocity of the center of mass agreed with the total impulse  $I = \int_0^{T_S} dt M_{bh} a_{bh}$  given, within errors which were taken to be the observed fluctuation in the center of mass velocity and acceleration of a galaxy with no kick (approximately 10%).

For BHs of mass  $10^8 M_\odot$ , slight to moderate asymmetries were induced in the dynamics of the host galaxy during the “on” phase, although nothing detectable was induced in the morphology, as illustrated in Figure 10. When viewed with the galaxy inclined to the line of sight, with the axis inclination aligned with the applied acceleration, deformations of the contours of constant radial velocity of order  $40 \text{ km s}^{-1}$  are clearly observed in the kinematics of the galaxy gas. Note that no grand-design spiral arms have formed in the stellar or gaseous components, ruling out density waves as a possible explanation for these. These streaming motions are also present when the line of sight is at other orientations to the line of sight, but are less prominent. These disk asymmetries disappeared when the acceleration was turned off, but the BH continued to oscillate about the center of mass with an amplitude that depended slightly on the initial acceleration, but was typically of order  $1 - 2 \text{ kpc}$ .

In the case where the BH is given an acceleration perpendicular to the galaxy plane, a similar behavior is observed, as illustrated in Figure 11. The BH oscillates around an equilibrium point, slowly dragging the galaxy along with it via dynamical friction. In this case, however, the amplitude of the motion is smaller and the frequency higher. The acceleration required for escape in this case is  $3.0 \times 10^{-8} \text{ cm s}^{-2}$ , as compared with 4.5 for the case in the plane of the galaxy. This case produces no detectably significant asymmetries in the morphology or kinematics of the galaxy disk.

#### 4.2. Black Hole Mass $10^9 M_\odot$

When given an acceleration in the plane of the galactic disk, the large  $10^9 M_\odot$  black hole exhibited behavior similar to that of the smaller hole. In this case, as illustrated in Figure 12, the larger impulse “drags” the galaxy a proportionally greater distance. When the acceleration is turned off after 0.2 Gyr, the velocity imparted to the galaxy is  $200 \text{ m s}^{-1}$ .

As the black hole was accelerated, it became displaced from the morphological and dynamical center of the galaxy, as illustrated in Figure 13. These induced asymmetries in the galaxy disk are more pronounced in this case than in the  $10^8 M_\odot$  case, in particular tending to drag the central regions of the galaxy with the movement of the



black hole via dynamical friction. In particular, while the BH in the first frame of Figure 13 appears displaced from the morphological center of the galaxy, the second frame of the figure illustrates how the dynamical center of the galaxy has been displaced towards the direction of acceleration of the black hole. The result is a characteristic “tongue–” shaped extension of the velocity contours on the side of the galaxy opposite the acceleration and flattened contours on the side of the galaxy in the direction of the acceleration. In test runs with a much larger, possibly unphysical  $10^{10} M_{\odot}$  BH, these features became associated with a central core region of the disk that moved along with the black hole, being more coupled to it than to the galaxy, and causing strong morphological asymmetries in the disk as the bulge was dragged off-center. We did not observe such strong asymmetric features in the morphology of the  $10^9 M_{\odot}$  galaxy, but do observe the “tongue” features that indicate that the BH is beginning to dominate the dynamics of the inner  $2 - 5$  kpc of the disk.

A similar behavior is observed when the acceleration is perpendicular to the plane of the galaxy. Again, streaming motions and dynamical asymmetries are observed for the first 0.5 Gyr of acceleration, as shown in Figure 14. Following that period, only slight streaming motions remain as part of the stabilized disk kinematics.

## 5. Discussion

We have analyzed the motions of massive black holes in the centers of galaxies which have received an impulsive kick (owing to the merging of two BHs) or received a sustained acceleration due to a one sided jet. We have studied the BH displacement from the galaxy center and the influence this has on the galaxy morphology and kinematics. An impulsive “kick” exceeding  $600 \text{ km s}^{-1}$  will ejects the BH from the galaxy. Accelerations of the order of  $4 \times 10^{-8} \text{ cm s}^{-2}$  or larger for times of the order of  $2 \times 10^8 \text{ yr}$  eject the BH from the galaxy. This acceleration is smaller than the Eddington limit on the one-sided jet luminosity (Tsygan 2007) by a factor of about 50.

For smaller velocity kicks or smaller sustained accelerations, the BH is observed to oscillate through the galaxy center for times of order Gyr.

The frequency of these oscillations decreases as the BH velocity kick increases or as the BH acceleration increases. In such galaxies, we can expect to observe central BHs which are offset from the centers of their host galaxy disks or have large radial velocity differences from their hosts. Larger mass BHs undergoing these oscillations induce streaming motions in their galaxies due to dynamical friction. This process may be a source of disk morphological and dynamical asymmetry in galaxies such as NGC 1637 or NGC 991 which exhibit nonaxisymmetries but are located in isolated fields far from potential sources of tidal interactions (Kornreich *et al.* 1998).

The asymmetries in the galaxy disk induced by the BH motion are of course more pronounced for more massive black holes. The BH tends to drag the central regions of the galaxy with it owing to dynamical friction. The dynamical center of the galaxy is seen some cases to be displaced towards the direction of the BH acceleration with a characteristic “tongue–” shaped extension of the velocity contours on the side of the galaxy opposite the acceleration.

As a check on the results, additional model runs with fewer ( $10^5$ ) or more ( $10^7$ ) particles yielded substantially similar behavior for the BH. Asymmetries induced in the galaxy disk remained qualitatively similar for each run, although the details of the locations and intensities of the induced asymmetries varied somewhat.

It is important to extend these studies to elliptical galaxies in the future. We expect that the results concerning conditions of BH escape from the galaxy will apply equally well there, as escape times from the disk are very short, of order 0.1 Gyr, and after that the gravitational potential is essentially that of the spheroidal halo.

We thank Martha Haynes and Larry Kidder for discussions. This work has made use of the computational facilities of the National Astronomy and Ionosphere Center, which is operated by Cornell University under a cooperative agreement with the National Science Foundation.

## REFERENCES

- Baldwin, J. E., Lynden-Bell, D., & Sancisi, R. 1980, MNRAS, 193, 313.

Bogdanović, T., Reynolds, C.S., & Miller, M.C. 2007, astro-ph/0703054v2

Campanelli, M., Lousto, C.O., Zlochower, Y., & Merritt, D. 2007, PRL, 98, 231102

Dickey, J. M., Hanson, M. M., & Helou, G. 1990, ApJ, 352, 522

González, J. A., Hannam, M. D., Sperhake, U., Bruegmann, B., & Husa, S., 2007, Phys. Rev. Lett., 98, 231101.

Kornreich, D. A., Haynes, M. P., & Lovelace, R. V. L., 1998, AJ, 116, 2154.

Landau, L. D., & Lifshitz, E. M. 1960, *Mechanics*, (Pergamon: Oxford), p. 29

Lovelace, R. V. E. 1976, Nature, 262, 649

Magain, P., Letawe, G., Courbin, F., Jablonka, P., Jahnke, K., Meylaan, G., & Wisotzki, L. 2005, Nature, 437, 381

Navarro, J. F., Frenk, C. S., White, S. D. M., ApJ, 462, 563.

Plummer, H. C., 1915, MNRAS, 76, 107.

Rownd, B. K., Dickey, J. M., & Helou, G. 1994, AJ, 108, 1638

Salpeter, E. E. 1964, ApJ, 140, 796

Shklovsky, I.S. 1982, in *IAU Symp. No. 97: Extragalactic Radio Sources*, Eds. D.S. Heeschen & C.M. Waade (Reidel: Dordrecht 1982), p. 475

Springel, V. 2005, MNRAS, 364, 1105

Tsygan, A.I. 2007, Astron. Repts., 51, 97

Wang, J.C.L., Sulkanen, M.E., & Lovelace, R.V.E. 1992, ApJ, 390, 46

Zaritsky, D., & Rix, H. 1997, ApJ, 466, 118.

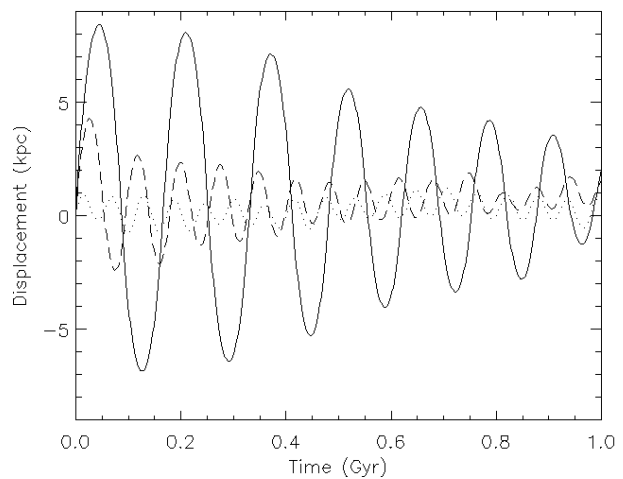


Fig. 7.— Motion along the direction of kick, in the plane of the galaxy, for the Black hole of mass  $10^9 M_\odot$  inside a model disk galaxy for an initial velocity kick of  $400 \text{ km s}^{-1}$  (solid line),  $300 \text{ km s}^{-1}$  (dashed line), and  $100 \text{ km s}^{-1}$  (dotted line).

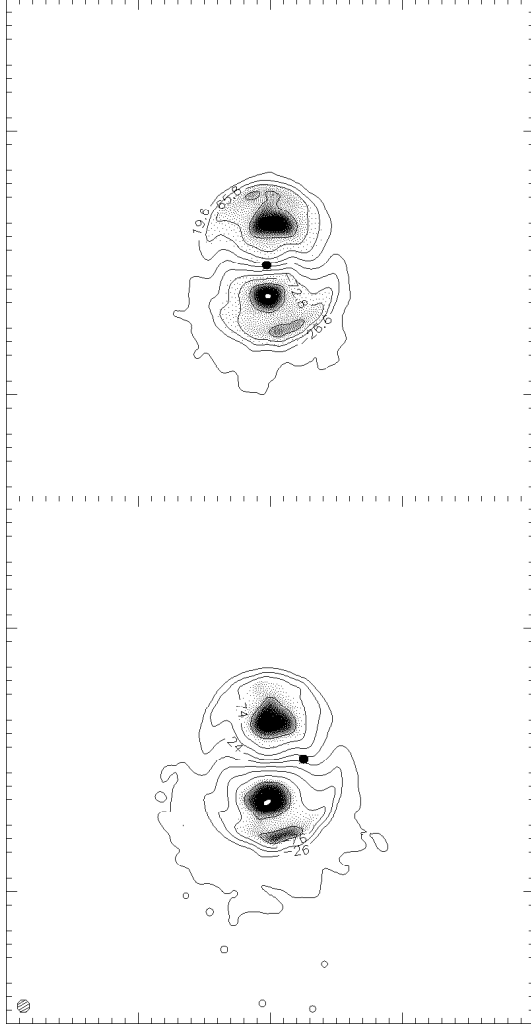


Fig. 8.— Kinematic asymmetries in the gas component of a galaxy with a  $10^9 M_\odot$  BH which has received an impulsive velocity kick. In the top panel, the kick velocity is  $200 \text{ km s}^{-1}$  to the right in the plane of the galaxy. The galaxy is inclined to the line of sight by  $30^\circ$ . The bottom panel is for the same parameters but for an initial velocity kick of  $400 \text{ km s}^{-1}$ . Contours of constant radial velocity are labeled in  $\text{km s}^{-1}$ . Major tick marks delineate 25 kpc.

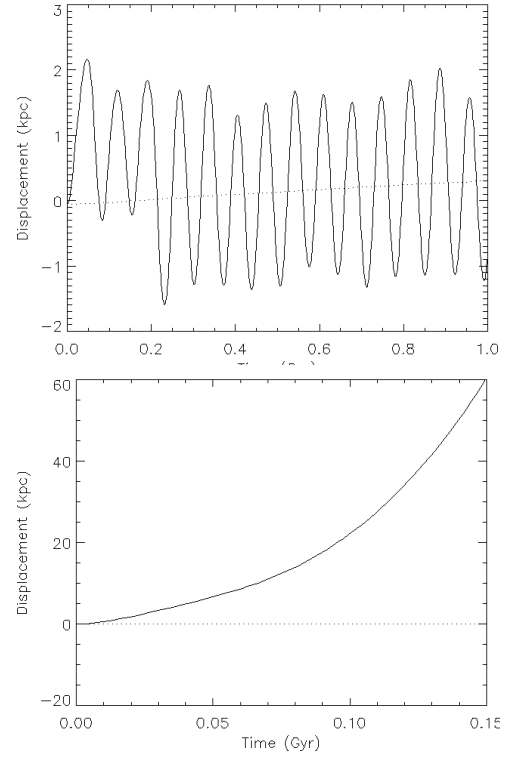


Fig. 9.— Displacement vs. Time along the direction of applied acceleration in the plane of the galaxy for a  $10^8 M_\odot$  black hole with simulated jet acceleration of  $2.0 \times 10^{-8} \text{ cm s}^{-2}$  for a time  $0 \leq t \leq 0.2 \text{ Gyr}$ . The dotted line shows the center of mass of the galaxy. The bottom panel shows the same quantities but for an acceleration  $4.0 \times 10^{-8} \text{ cm s}^{-2}$ .

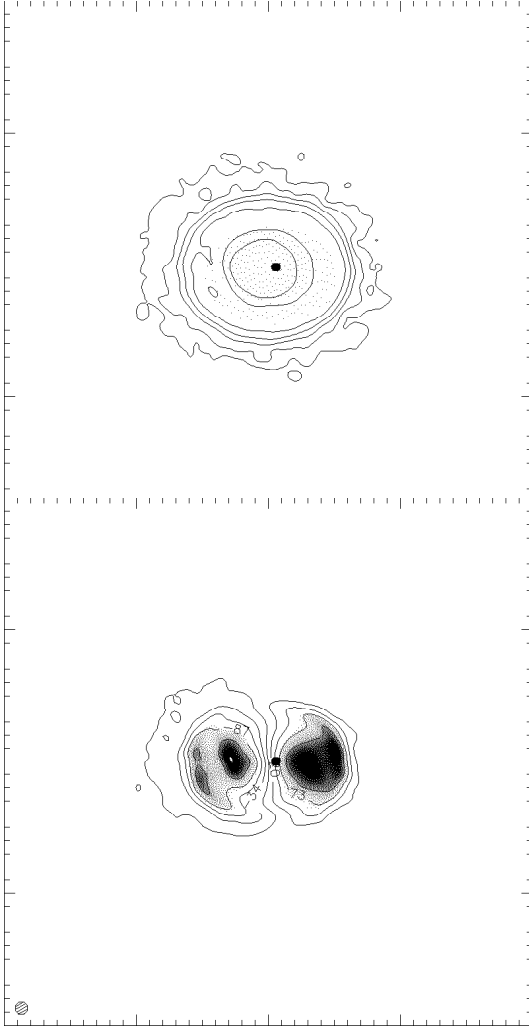


Fig. 10.— Galaxy model gas density contours and velocity map, convolved with a simulated Gaussian telescope beam, for the  $10^8 M_\odot$  BH with an applied acceleration of  $2.0 \times 10^{-8} \text{ cm s}^{-2}$  at time  $t = 0.2 \text{ Gyr}$ . The inclination to line of sight is  $30^\circ$  about the axis of acceleration. Major tick marks delineate 25 kpc.

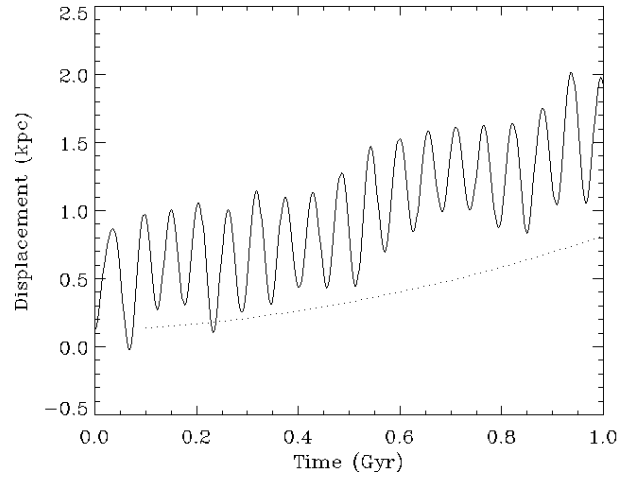


Fig. 11.— The BH displacement as a function of time along the direction of the applied acceleration perpendicular to the plane of the galaxy for a  $10^8 M_\odot$  black hole. The simulated jet acceleration is  $2.0 \times 10^{-8} \text{ cm s}^{-1}$ . The dotted line shows the center of mass of the galaxy.

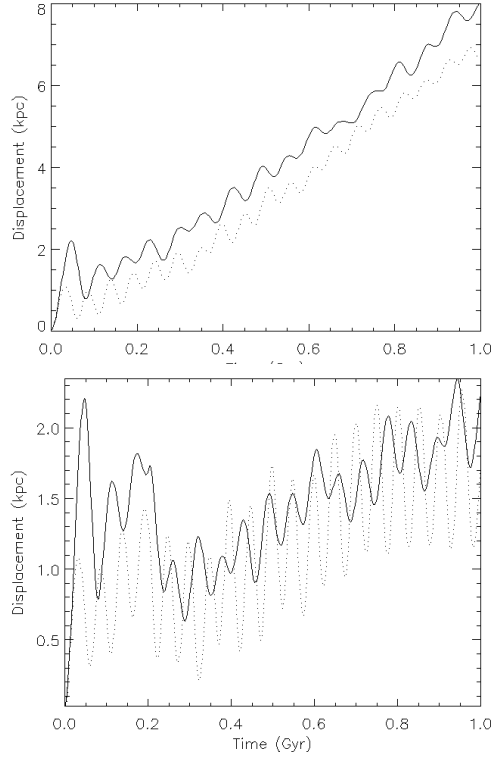


Fig. 12.— Displacement vs. Time along the direction of applied acceleration for the black hole of mass  $10^9 M_\odot$  with simulated jet acceleration of  $2.0 \times 10^{-8} \text{ cm s}^{-2}$ . Acceleration in the plane of the galaxy is represented by the solid line; perpendicular to the plane by the dotted line. In the bottom panel, the acceleration has been shut off at 0.2 Gyr.

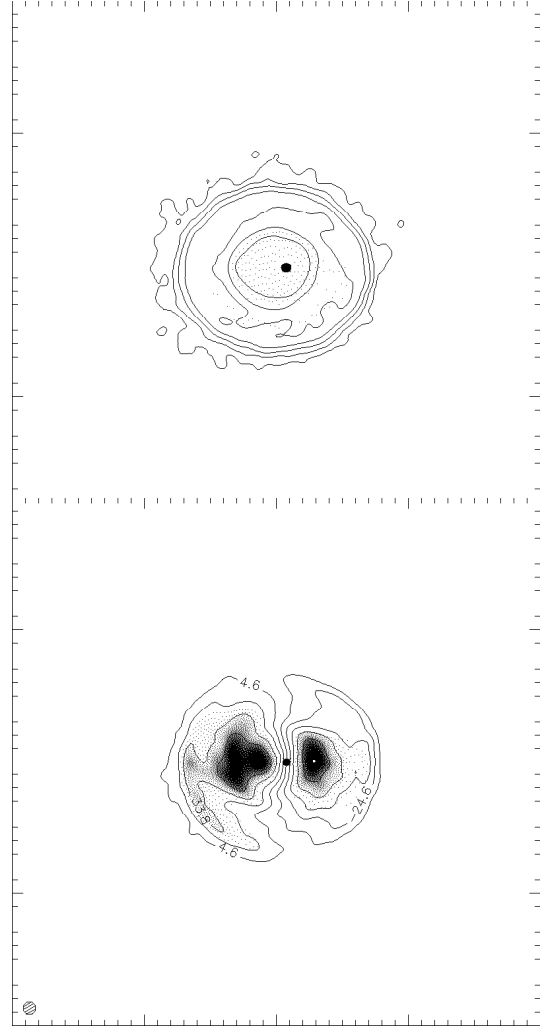


Fig. 13.— Galaxy model gas density contours (top panel) and velocity map (bottom panel), convolved with a simulated Gaussian telescope beam, for the case of a  $10^9 M_\odot$  black hole with an applied acceleration of  $2.0 \times 10^{-8} \text{ cm s}^{-2}$  in the plane of the galaxy, at time  $t = 0.2 \text{ Gyr}$ . The inclination to line of sight is  $30^\circ$  about the axis of acceleration. Major tick marks delineate 25 kpc.

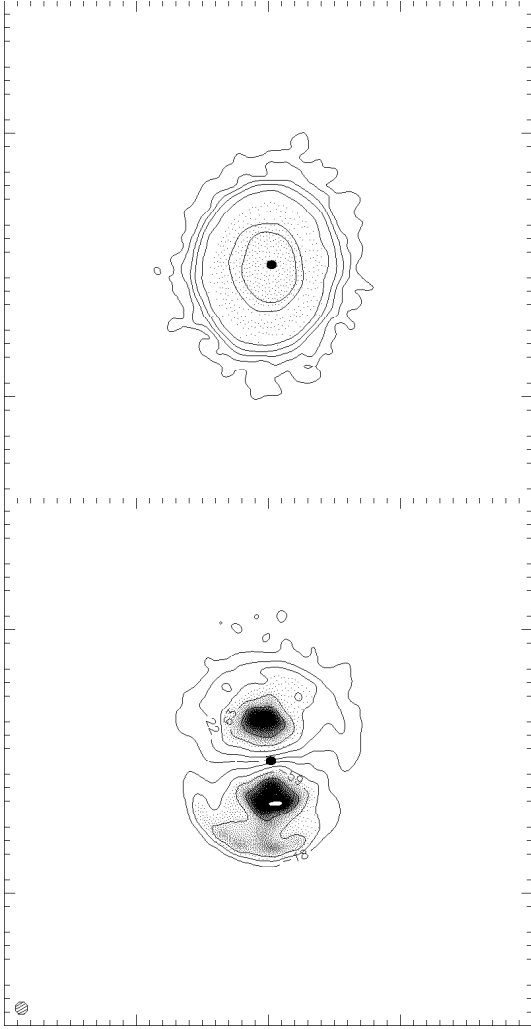


Fig. 14.— Gas density contours (top panel) and velocity map (bottom panel), convolved with a simulated Gaussian telescope beam, for the case of a  $10^9 M_\odot$  black hole with an applied acceleration of  $2.0 \times 10^{-8} \text{ cm s}^{-1}$ , perpendicular to the plane of the galaxy at time  $t = 0.2 \text{ Gyr}$ . The inclination to the line of sight is  $30^\circ$ . Major tick marks delineate 25 kpc.